J Oceanogr (2015) 71:65–75
DOI 10.1007/s10872-014-0260-6

ORIGINAL ARTICLE

A highly sensitive and large concentration range colorimetric continuous flow analysis for ammonium concentration

Taketoshi Kodama · Tadafumi Ichikawa · Kiyotaka Hidaka · Ken Furuya

Received: 9 July 2014 / Revised: 7 October 2014 / Accepted: 14 November 2014 / Published online: 26 November 2014
© The Oceanographic Society of Japan and Springer Japan 2014

Abstract A continuous flow method for the determination of ammonium concentration in seawater from a nanomolar to a micromolar level is described. To prevent spurious peaks derived from salinity difference, a gas-permeable hydrophobic membrane filter was used to separate the manifold into an outgassing section and an indophenol blue reaction section. The indophenol blue reaction section was adopted for colorimetric analysis and is equipped with a 1-m path length liquid capillary cell and a fiber-optic spectrometer, which is able to record the absorbance at multiple wavelengths. The minimum detection limit at wavelength 630 nm is 5.5 ± 1.8 nM, and the calibration curves are linear to at least 2,000 nM. In addition, the minimum detection limit at wavelength 530 nm was 13 ± 5.3 nM, and linear calibration curves were observed until at least 10,000 nM. The slopes of the calibration curves were similar for standards prepared using filtered seawater and ultrapure water. The ammonium concentration of the ultrapure water was similar to those of ion-exchanged water and unfiltered low-nutrient seawater, but was significantly lower than those of filtered seawater and solutions that contained sodium hydroxide. Therefore, ultrapure water is optimal for both blank and standard preparations because of its stable quality and availability. Given its large concentration range and the use of readily available blanks, this method is suitable for the determination of ammonium concentration and helps our understanding of ammonium dynamics in the ocean.

Keywords Ammonia · Ammonium ion · Nanomolar level · Liquid waveguide capillary cell · Salt effect · Highly sensitive · Nitrogen dynamics · Autoanalyzer

T. Kodama · T. Ichikawa · K. Hidaka
National Research Institute of Fisheries Science, Fisheries Research Agency, Fukuura, Kanazawa, Yokohama, Kanagawa 236-8648, Japan

Present Address:
T. Kodama (✉)
Japan Sea National Fisheries Research Institute, Fisheries Research Agency, 1-5939-22, Suido-cho, Chuou-ku, Niigata, Niigata 951-8121, Japan
e-mail: takekodama@affrc.go.jp

K. Furuya
Department of Aquatic Bioscience, The University of Tokyo, Yayoi, Bunkyo, Tokyo 113–8657, Japan

1 Introduction

Ammonium (ammonium ion + ammonia) present in the surface layer of the ocean is important for biological productivity. Ammonium is the most preferred nitrogen source for uptake by phytoplankton (Dortch 1990), and ammonium uptake is 2–3 times higher than nitrate uptake (Eppley and Peterson 1979; Rees et al. 2006; Clark et al. 2007). Heterotrophic bacteria assimilate ammonium (Wheeler and Kirchman 1986), and a type of Archaea and other bacteria have the ability to oxidize ammonia and utilize ammonium as an energy source (Francis et al. 2005; Ward 2011). Although the ammonium concentration is sometimes elevated to several micromolar in the ocean (Karl et al. 1992; Nishino et al. 2011), it is generally low. Usually, the concentration is less than 0.5 μM because of active uptake by plankton (Saino et al. 1983; Kirchman et al. 1990), and in oligotrophic oceans it is depleted to less than several tenths of a nanomolar (Brzezinski 1988; Lipschultz 2001).

The most popular technique for ammonium determination during oceanic observations is colorimetry based on the indophenol reaction (Parsons et al. 1984; Li et al. 2005;

McCarthy and Bronk 2008). Previously, the measurement of submicromolar ammonium concentrations was difficult because of high contamination levels and low sensitivity (Li et al. 2005; Parsons et al. 1984). Therefore, highly sensitive ammonium analyses with detection limits less than 10 nM were developed in the last quarter of a century (Ma et al. 2014; O'Connor Šraj et al. 2014). These methods are either colorimetric, based on the formation of indophenol blue (Brzezinski 1987; Li et al. 2005; Chen et al. 2011; Zhu et al. 2014) or fluorometric, based on the reaction of ammonium with *o*-phthaldialdehyde (Jones 1991; Kerouel and Aminot 1997; Amornthammarong and Zhang 2008). Fluorometric methods are sometimes applied to nanomolar level ammonium detection during oceanic observations (e.g., Lipschultz 2001; Matsumoto et al. 2004; Rees et al. 2006; Raimbault and Garcia 2008; Raimbault et al. 2008). However, indophenol blue methods for oligotrophic oceanic observations are quite limited (Brzezinski 1988; Harrison et al. 1996; Li et al. 2005; Zhu et al. 2014), although the methods have been further developed.

One of the problems with the indophenol blue method is finding an appropriate blank for the ammonium measurement. In highly sensitive analytical methods for nitrate, phosphate, and silicate, the blank is typically ultrapure water (Garside 1982), seawater with the target nutrient removed via coprecipitation (Karl and Tien 1992; Li and Hansell 2008; Patey et al. 2008; Hashihama et al. 2009; Hashihama and Kanda 2010), or water with a target nutrient concentration determined using ultrapure water as a blank (Patey et al. 2008; Hashihama et al. 2009). However, for ammonium determination using indophenol blue methods, seawater collected in an oligotrophic ocean (Brzezinski 1987, 1988) or seawater with added sodium hydroxide that has been heated at 60 °C (Li et al. 2005) is typically used as the blank. While the ammonium concentration in surface seawater, determined using the fluorescence method, is as low as ultrapure water (Jones 1991), it is doubtful that the ammonium concentration in this blank is uniform. This is because ammonium concentrations in surface seawater are not stable in the subtropical gyre (Lipschultz 2001). The treated seawater used by Li et al. (2005) was likely contaminated during handling (i.e., during filtration).

While ultrapure water is a suitable blank, it is not used because most indophenol blue methods are generally not free of the salt effect. However, Zhu et al. (2014) report that the salt effect was negligible in their system. In contrast, Li et al. (2005) showed that the ammonium concentration was increased by increases in salinity. Furthermore, salinity differences in the sample matrix cause spurious peaks, which make accurate analysis difficult (Coverly et al. 2012). Chen et al. (2011) reported a highly sensitive indophenol blue method, which is free from the salt effect and uses ultrapure water as the blank solution. However, this method requires complex equipment for online solid-phase extractions. Moreover, the measurement time (20 min per sample) is too long for application to routine oceanic analyses, and; hence, unsuitable, because the ammonium concentration of the samples should be determined within a few hours after collection (Hydes et al. 2010). Gas diffusion is a promising technique to eliminate the salt effect (Oliveira et al. 2009); however, this highly sensitive technique was only reported with a conductometric method with a detection limit of 10 nM (Plant et al. 2009).

A narrow detection range is another problem with the highly sensitive colorimetric and fluorometric methods. In the ocean, the ammonium concentration varies from several nanomolar to micromolar values (vide supra), but the maximum linear detection limits are less than 2 μM with highly sensitive methods (Brzezinski 1987; Jones 1991; Kerouel and Aminot 1997; Li et al. 2005; Amornthammarong and Zhang 2008; Chen et al. 2011). Therefore, we developed a quick and highly sensitive ammonium determination method, which is accurate over a wide range of concentrations and is largely independent of salinity effects. This method relies on a gas diffusion technique (Van Son et al. 1983), and only requires a liquid waveguide capillary cell (LWCC). The LWCC can be attached to an existing continuous flow autoanalyzer, which is a popular method for highly sensitive nutrient analyses (Li et al. 2005; Patey et al. 2008).

2 Experimental

2.1 Automated analytical system

A gas-segmented continuous flow colorimeter (AAII, Bran + Luebbe) was employed for the automated low-level determination of ammonium in seawater (Fig. 1). The manifold configuration and flow diagram were modified from the report by Van Son et al. (1983); the reagents and their flow rates were also changed. The manifold was separated into two sections: an outgassing section, and an ingassing and indophenol reaction section. In the outgassing section, the sample solution was mixed with an alkaline solution containing ethylenediaminetetraacetic acid (EDTA) and flows through glass coils. Elevation of the pH in the presence of the chelating agent EDTA resulted in the formation of ammonia (gas) from the ammonium ions in the sample without precipitation of hydroxide salt. The ammonia gas was absorbed by a sulfuric acid solution in a gas diffusion unit (Fig. 1). The gas diffusion unit consisted of a PTFE gas-permeable membrane filter (pore size = 0.5 μm, thickness = 0.075 mm, T050A090C, ADVANTEC) and a dialyzer. The pH was measured using an electronic pH meter (M-12, Horiba). The residence time for the ingassing and

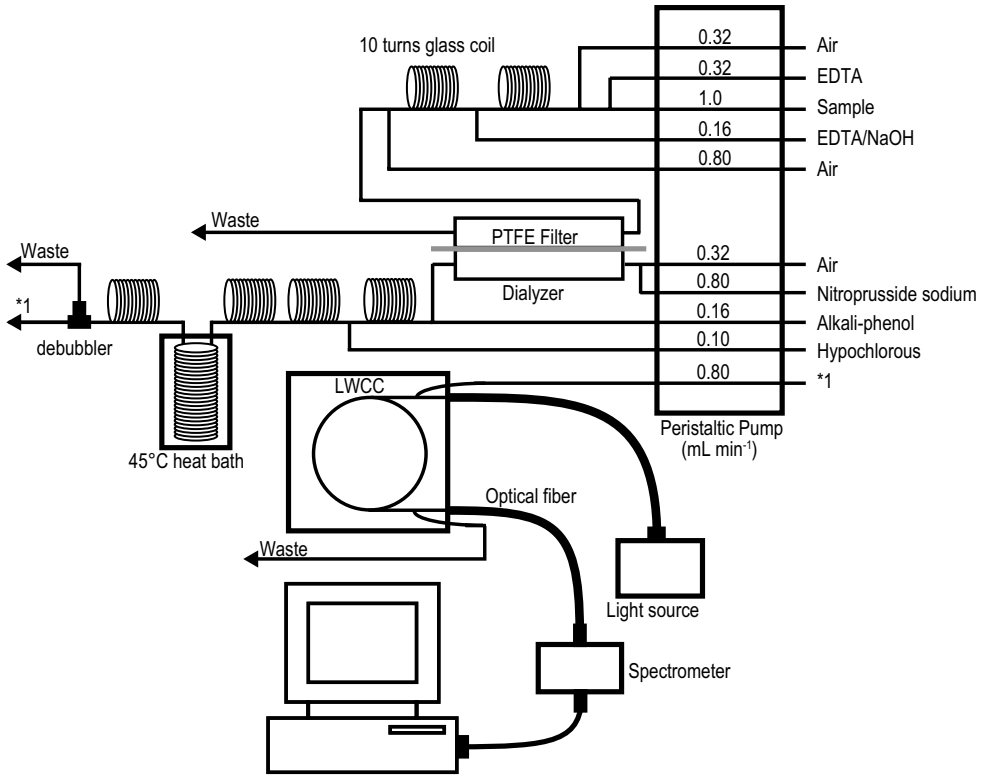

Fig. 1 Manifold configuration and flow diagram for the gas-segmented continuous flow analysis of trace ammonium using an LWCC

outgassing sections of the dialyzer was 7 s and 16 s, respectively. The ammonia absorbed in the acid solution reacted with alkali-phenol and hypochlorite solutions in a 45 °C bath to generate indophenol blue dye. After the segmented gas was removed from the waste line (Fig. 1), the intensity of light transmitted through the reacted solution was detected using a 1-m path length LWCC (LWCC-2100, World Precision Instruments), a fiber optic tungsten light source (FO-6000, World Precision Instruments), optical fibers (P-200-2-UU/VIS, Ocean Optics), and a fiber-optic spectrometer (USB4000, Ocean Optics). The spectrometer was connected to a personal computer using the SpectraSuite software (Ocean Optics).

According to the Lambert–Beer's law, absorbance was calculated using the following equation:

$$A_\lambda = -\log_{10}\left(\frac{S_\lambda - D_\lambda}{R_\lambda - D_\lambda}\right). \quad (1)$$

In this equation, A_λ and S_λ are the absorbance and light intensity observed through the sample with the added reagents at a wavelength of λ nm, respectively. D_λ and R_λ are the dark intensity and reference intensity at a wavelength of λ nm, respectively. In the present study, the highest absorbance and the most sensitive measurements with indophenol blue were obtained at a wavelength of 630 nm. Low sensitivity values were obtained for a

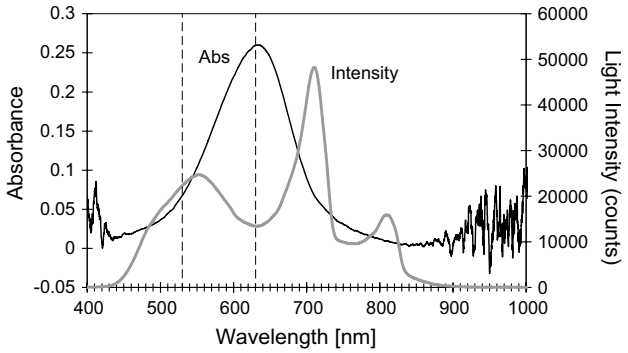

Fig. 2 Typical absorbance (*black line*) and transmitted light intensity (*gray line*) for ammonium at wavelengths between 400 nm and 1000 nm. The *horizontal dashed lines* denote the obtained wavelength of 530 and 630 nm

wavelength of 530 (Fig. 2). The values of D_{630} and D_{530} were set at zero in the present study because the SpectraSuite software can correct the electric dark to zero when a USB4000 spectrometer is used. The values of R_{630} and R_{530} equal the light intensity through ultrapure water containing reagents. In the present study, the value of R_{630} and R_{530} were adjusted by changing the integration time (the frequency of the measurement) because the light source intensity cannot be adjusted and the transmitted

light intensity (S_λ and R_λ) cannot be measured for values higher than 65,500 counts using a USB4000. S_{630} and S_{530} were recorded and outputted at least once per second during the measurement.

2.2 Analytical reagents

All the chemicals used in this study were reagent grade and were dissolved in ultrapure water purified using an ultrapure water system (AQUARIUS, Advantec). The concentrations of the following reagents were prepared manually.

2.2.1 30 % Triton-X solution

Triton-X 100 (Sigma, 30 mL) was dissolved in ultrapure water (70 mL) and ultrasonicated for 20 min at room temperature.

2.2.2 EDTA (0.28 M EDTA/0.065 M H_3BO_3) reagent

EDTA·4Na (Dojindo 62.5 g) and boric acid (Wako 2.0 g) were dissolved in ultrapure water (ca. 400 mL) and then diluted to 500 ml in a measuring flask. The 30 % Triton-X solution (2.5 mL) was then added to the EDTA mixture. The mixing ratio of this reagent to the sample solution was 0.32:1.

2.2.3 EDTA/NaOH (0.18 M EDTA/1.25 M NaOH) reagent

EDTA·4Na (16 g) and sodium hydroxide (Wako 10 g) were dissolved in ultrapure water (ca. 150 mL), and then the solution was diluted with ultrapure water in a measuring flask to 200 mL. The mixing ratio of this reagent to the sample was 0.16:1.

2.2.4 Nitroprusside (0.67 mM nitroprusside sodium/0.01 M H_2SO_4) reagent

A 1 M H_2SO_4 stock reagent was first prepared by dissolving sulfuric acid (Wako 5.6 mL) in ultrapure water (95 mL). An 8.4 mM nitroprusside sodium reagent was then prepared by dissolving nitroprusside sodium (Wako 0.25 g) and 1 M H_2SO_4 (0.20 mL) in ultrapure water (100 mL). These stock reagents were stored in the dark at 4 °C. A working solution was prepared by adding 1 M H_2SO_4 (5.0 mL) and the stock nitroprusside sodium reagent (4.0 mL) to ultrapure water (500 mL) followed by the 30 % Triton-X solution (1.0 mL). The reagent suction rate in the flow line was 0.80 mL min^{-1} when the sample suction rate was 1.0 mL min^{-1}, and the ratio of the flow volumes at the outgassing and ingassing sections in the dialyzer was 1:0.43.

2.2.5 Alkali-phenol (0.53 M phenol/0.039 M citrate/0.625 M NaOH) reagent

First, sodium hydroxide (Wako 5.0 g) was dissolved in ultrapure water (200 mL). After cooling, trisodium citrate dehydrate (Wako 2.0 g) and solid phenol (Wako 10.0 g) were dissolved in the sodium hydroxide solution. This solution could be stored for at least 1 week at 4 °C. The mixing ratio of this reagent to the nitroprusside reagent was 1:5.

2.2.6 Hypochlorous reagent

Liquid sodium hypochlorite (Dojindo 5 mL) with an available chlorine concentration greater than 5.0 % was mixed with ultrapure water (100 mL). This reagent was prepared daily. The mixing ratio of this reagent to the nitroprusside reagent was 1:8.

2.3 Standards and blanks

An ammonium stock standard solution (1 L, 10 mM) was prepared from ammonium sulfate (analytical reagent grade) that was pre-dried (110 °C for 2 h) and stored in the dark at 4 °C after adding one drop of chloroform. In accordance with Li et al. (2005), working standards from 5 nM to 10,000 nM were prepared in polypropylene measuring flasks (100 mL or 200 mL) using both ultrapure water and low-nutrient seawater (LNSW). The LNSW was collected at 30°N, 138°E of the oligotrophic western North Pacific in October 2009, and stored for more than 1 year in light at room temperature.

Blank solutions included ultrapure water with a conductivity less than 0.06 μS cm^{-1}, ion-exchanged water with a conductivity less than 0.1 μS cm^{-1}, a 0.625 M sodium hydroxide solution heated overnight at 65 °C (NaOH aq.), a 3.5 % (0.060 M) sodium chloride aqueous solution, and 0.2-μm filtered and unfiltered LNSW. The filtered LNSW was collected and stored in the same manner as the unfiltered LNSW. In addition, according to Li et al. (2005), a blank was also prepared by adding 0.625 M sodium hydroxide (1 mL) to the LNSW supernatant (9 mL) and heating overnight at 65 °C (alkaline-LNSW).

2.4 Cleaning and maintenance

Before and after daily use, the reaction path in the manifold and the LWCC were cleaned using a 1 % Triton-X 100 aqueous solution. In this study, the precipitation of hydroxide salt was prevented via the addition of EDTA. However, precipitates were deposited in the reaction path when EDTA concentrations were lower than normal because of issues with flow lines, such as when the pump tube was broken. These precipitates were readily removed by rinsing

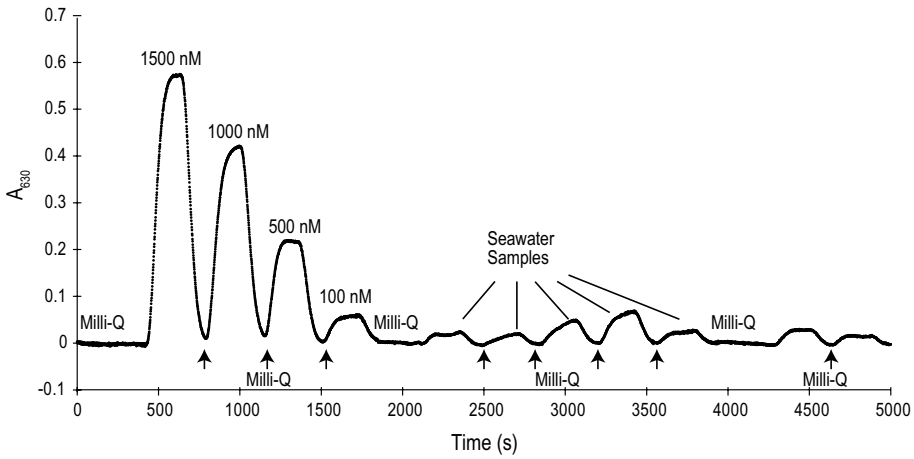

Fig. 3 Typical output signals for ammonium from the flow analyzer equipped with an LWCC. Ultrapure water was injected for the first 450 s, and then working standards of various ammonium concentrations prepared using ultrapure water and seawater samples collected in the oligotrophic western Pacific were sequentially injected for 210 s, with ultrapure water injected for 150 s in the intervening periods

with 6 M HCl. In addition, introduction of 6 M HCl via suction through the hypochlorous reagent and alkali-phenol reagent lines was effective for cleaning the LWCC. The PTFE membrane filter generally remained in good condition for at least 2 weeks; however, it was changed every 2 weeks. The signal for filter deterioration was the length of the gas-segmented patterns, which was different before and after the dialyzer when the filter had deteriorated.

3 Results and discussion

3.1 Linear dynamic range and detection limit

A typical output signal for nanomolar concentrations of ammonium was derived from analyses using the gas-segmented flow injection analyzer equipped with the LWCC (Fig. 3). Coverly et al. (2012) reported that spurious peaks were formed when the matrix changed from freshwater to seawater because of the salinity difference; however, spurious peaks were not observed in this study (Fig. 3). Therefore, the hydrophobic PTFE membrane filter was considered able to prevent the transport of ions, which was consistent with Oliveira et al. (2009). To determine the optimum sample suction time for the 400 nM working standard, the time was varied from 30 s to 240 s. A sample suction time of 180 s was found to be sufficient for reaching 95 % of the maximum absorbance, which is the 10 s mean absorbance at the top of the 240 s suction using this system (Fig. 4). The peak shapes also indicated that a sample suction of 180 s was sufficient for reaching maximum absorbance. Therefore, sample and wash times greater than 180 s were considered to be effective for eliminating the influence of sample dispersion. An acceptable carryover coefficient of 0.2 % was obtained when the sample suction intervals were set to 360 s; the coefficient for well-designed and maintained channels is <0.3 % (Gordon et al. 1993).

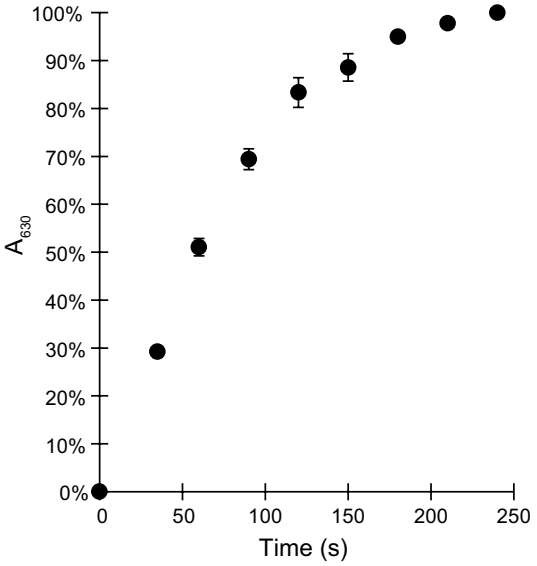

Fig. 4 Percentage of output signal for 400 nM ammonium standards as a function of sample suction duration. *Error bars* indicate the standard deviation ($n = 3$)

Therefore, the treatment capacity of the system (10 samples per hour) and the sample volume (3.0 mL) were suitable for achieving accurate analysis results. However, this treatment capacity was lower than the previous method (22 samples per hour; Zhu et al. 2014).

A calibration curve for A_{630} (the absorbance at 630 nm) was established using triplicate measurements of ten different concentrations of working standards from 0 nM to 2,000 nM, which were prepared using ultrapure water (Fig. 5a). A linear absorbance response to trace ammonium concentrations ≤2,000 nM were obtained with a significant correlation ($r^2 = 0.9993$). In addition, working standards up to 200 nM also provided a linear absorbance response ($r^2 = 0.9956$, Fig. 5b). The day-to-day slope variations ranged from 4.0×10^{-4} to 5.8×10^{-4} (mean ± SD

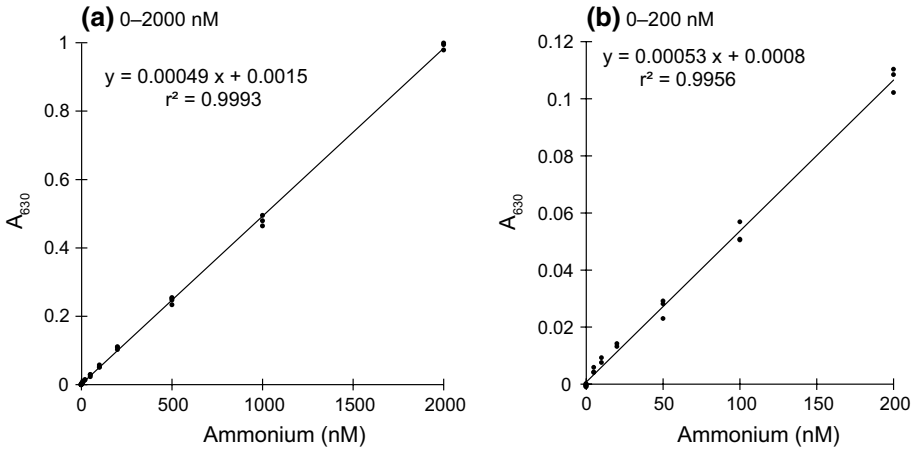

Fig. 5 Linearity of ammonium concentration at A_{630} **a** from 0 nM to 2000 nM and **b** from 0 nM to 200 nM using the highly sensitive continuous flow analysis

Table 1 Comparison of detection ranges and blanks for other highly sensitive systems

Detection method	Detection limit (nM)	Linear range (nM)	Matrix used as blank	References
Colorimetry	3.5	5–400	Seawater	Brzezinski (1987, 1988)
	5	10–1,000	Seawater added NaOH	Li et al. (2005)
	3.5	3.5–428	Ultrapure water	Chen et al. (2011)
	3.6	10–30,000	Not described	Zhu et al. (2014)
	5.5	5–10,000	Ultrapure water/seawater	This study
Fluorometry	1.5	5–150	Seawater	Jones (1991)
	1.5	20–100	Ultrapure water	Kerouel and Aminot (1997)
	1	5–1,000	Ultrapure water	Amornthammarong and Zhang (2008)
Conductometric	10	10–2,000	Seawater	Plant et al. (2009)

$4.9 \times 10^{-4} \pm 0.7 \times 10^{-4}$, $n = 6$). However, the slope variations were not stable, and the exact causes for these variations are not clear; the age-related degradation of the filter, and the differences in the working reagents may affect the variations. The minimum detection limits were 2.3–7.6 nM (5.5 ± 1.8 nM, $n = 6$), which was estimated to be three times the standard deviation of the measurement blank (ultrapure water; $n = 5$; Miller and Miller 1988). The variation of the detection limit in this study was due to variations in the day-to-day slope. Our lowest detection limit (2.7 nM) was the lowest of all reported for high sensitive colorimetric methods and higher than those for the fluorometric methods (Table 1). On the other hand, the highest detection limit (7.6 nM) was the highest of the previously reported highly sensitive analysis except for the conductometric method using a PTFE filter (Plant et al. 2009). The reproducibility of the 100 nM standards had a coefficient of variation of 3.8 % ($n = 5$), which is lower than the previous studies using the indophenol blue methods (5 %; Li et al. 2005 and 4.4 %; Zhu et al. 2014). Therefore, detection of trace ammonium concentrations with high precision was achieved using this LWCC system.

However, the maximum detection limit was not high enough for application to oceanic observations, because

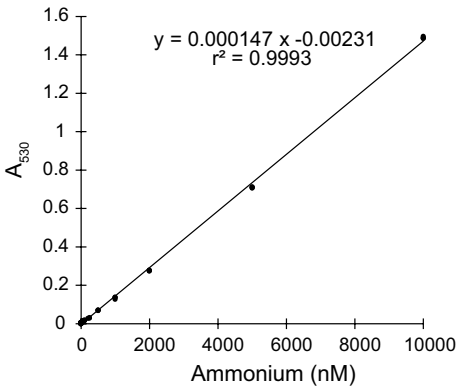

Fig. 6 Linearity of ammonium concentration at A_{530} using the highly sensitive continuous flow analysis

the ammonium concentration in the ocean may be several micromolar (Jones 1991; Karl et al. 1992; Nishino et al. 2011). Thus, the A_{530} values, which have a lower sensitivity than the A_{630} values were concurrently measured with A_{630} values using the same settings. As a result, a significant linear absorbance response to ammonium concentrations ≤10,000 nM was obtained using the calibration curve for A_{530} ($r^2 = 0.9993$, Fig. 6). The daily slope variation

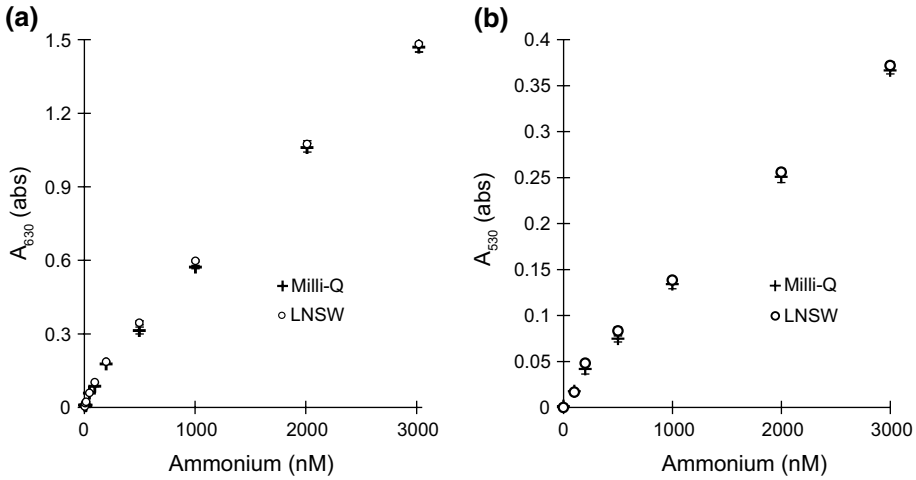

Fig. 7 Comparison of ammonium concentration in working standards prepared using ultrapure water (*crosses*) and unfiltered LNSW (*open circles*) at **a** A_{630} and **b** A_{530}. Each working standard was measured three times, and the *bars* denote the standard deviation. The value of D_λ was set as "0."

ranged from 1.21×10^{-4} to 1.48×10^{-4} (mean ± SD $1.42 \times 10^{-4} \pm 1.1 \times 10^{-5}$, $n = 6$). The minimum detection limit of 13.0 ± 5.3 nM ($n = 6$) was too high to determine ammonium concentrations at nanomolar levels; however, this was not a critical problem because low-level ammonium concentrations were measured with A_{630} values. The molar absorptivity values at 630 nm and 530 nm were 8.7×10^3 and 1.4×10^3 $M^{-1}cm^{-1}$, respectively.

3.2 The salt effect and the blank

Ten different concentrations of working standards from 5 nM to 3,000 nM were prepared using ultrapure water and filtered LNSW (Fig. 7). The relationship between A_{630} and the standards was nonlinear, because the A_{630} value for the 3,000 nM standards was beyond the upper limit of the detection range. The values of both A_{630} and A_{530} were not generally different between freshwater and seawater ($n = 3$; Fig. 7), although significant differences were obtained for the 50 nM and 500 nM standards (t test, $p < 0.05$). The A_{630} values for the 50 nM and 500 nM standards and A_{530} values for the 500 nM standards were higher than those estimated by linear regression; thus, contamination may have occurred in these two standards. Plant et al. (2009) reported that salinity has an effect on ammonium diffusion, and the ammonium transit in the diffusion cell (dialyzer in this study) decreased by 12 % for the seawater compared with the ultrapure water because of the pH difference. The ammonium diffusive flux (J) through the PTFE membrane is derived from the following equation (Schulze et al. 1988):

$$J = k \times D \times (A/L) \times \Delta c, \quad (2)$$

where, k, D, A, L, and Δc are the lump constant, the contact area between the outgassing and ingassing sections, the membrane thickness, the diffusion coefficient of ammonia in air, and the ammonia concentration gradient, respectively. The membrane thickness (A) in this study was suitable for the gas diffusion method according to Plant et al. (2009). In Eq. 2, Δc is theoretically different between seawater and ultrapure water, because the pH difference causes the conversion of ammonium ion to ammonia. This difference in the pH of ultrapure water (theoretically 7, but usually less) and seawater (8.32) is significant. In the present system, the pHs of the seawater with added reagents and the ultrapure water with added reagents were 11.98 ± 0.012 and 11.77 ± 0.004 (both $n = 5$), respectively. The acid dissociation constant of ammonium/ammonia (K_a) is 5.6×10^{-10} (Dean 1998); thus, the ammonium/ammonia in the samples existed as 99.7 % and 99.8 % ammonia in the seawater and ultrapure samples, respectively. This difference was rarely detected for the current method. In addition, the hydrophobic membrane filter generally prevents the transport of ions from samples containing EDTA to the nitroprusside reagent (Oliveira et al. 2009). Therefore, ultrapure water can be used as the blank solution and for preparation of the standards.

The ammonium concentration in ultrapure water was assumed to be "zero" in previous studies (Table 1). The conductivity of pure water is theoretically 0.055 μS cm^{-1} (Dean 1998), while the conductivity of ultrapure water used in this study was less than 0.06 μS cm^{-1}. The specific electrical conductance of ammonium and hydroxide ions is 53.5 and 198 S cm^2 $equiv^{-1}$ at 25 °C, respectively, and K_a is 5.6×10^{-10} (Dean 1998). When only ammonium contamination is assumed to increase the conductivity of pure water from the theoretical value to a practical value (<0.01 μS cm^{-1}), the ammonium concentration for ultrapure water would be less than 0.05 nM, which is much lower than the detection limit and can be ignored. Therefore, the ammonium concentration in the ultrapure water was considered as 0 nM. In addition, the ammonium concentration in the ion-exchanged water (conductivity <0.1 μS cm^{-1}) is theoretically less than 0.4 nM, and the measured ammonium

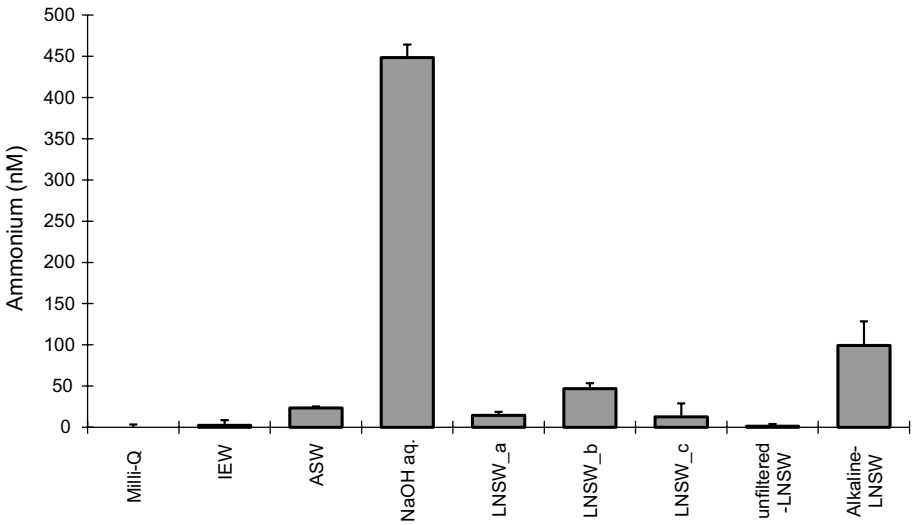

Fig. 8 Comparison of the ammonium concentration in the favored blank solutions. *Error bars* indicate the standard deviation ($n = 4$)

concentration in ion-exchanged water was not significantly different from ultrapure water (Fig. 8).

The ammonium concentration in unfiltered LNSW was lower than the detection limit (<2.3 nM) and not significantly higher than ultrapure water (Fig. 8). On the other hand, the ammonium concentration in filtered LNSW differed between batches (LNSWs: a–c in Fig. 8), while the concentration in all batches was significantly higher than ultrapure water. The ammonium concentration in ASW was also higher than ultrapure water. The ammonium concentrations in the 0.625 M NaOH aq. solution and the alkaline-LNSW were 448 ± 15.8 nM and 99 ± 29.3 nM, respectively (Fig. 8). These results indicate that ultrapure water, ion-exchanged water, and unfiltered LNSW are suitable for use as blank solutions. Furthermore, ultrapure water is considered to be the best blank solution for use with this method because of its stability, economics, and ease of handling. Since the ammonium concentration in the 0.625 M NaOH aq. solution and the alkaline-LNSW (Fig. 8) were high, NaOH is the source of the ammonium contamination. The EDTA/NaOH and alkali-phenol reagents can also contaminate ammonium, which decreases the light intensity (S_λ and R_λ) and sensitivity of the analysis. Therefore, the NaOH used for preparing reagents in this study was as new as possible in order to minimize contamination.

3.3 Interference study

To assess the possibility of interference with ammonium determination, solutions containing 10 mM urea ($(NH_2)_2CO$) and glycine (aminoacetic acid NH_2CH_2COOH) in ultrapure water were prepared, and their absorbance was measured. The absorbance of the aqueous 10 mM urea and glycine solutions was significantly higher than ultrapure water, with indicated ammonium concentrations of 2,277 ± 34.6 nM and 98 ± 10.0 nM, respectively (both $n = 4$). However, in open and coastal oceans the concentrations of urea and dissolved free amino acids are generally lower than 1 µM (Bronk 2002), and the absorbance of urea and glycine solutions at 1 µM are 0.23 and 0.098 nM of ammonium concentrations, respectively.

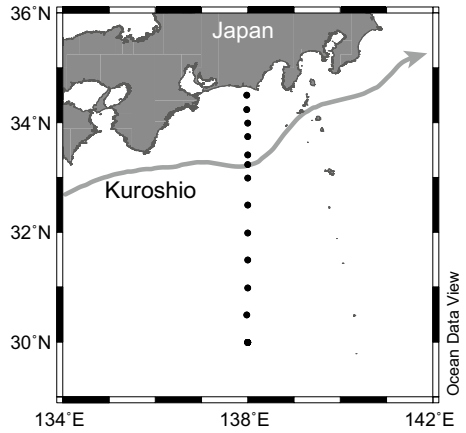

Fig. 9 Stations where the highly sensitive ammonium determination system was applied in the south of Japan. The *arrow* indicates the position of the Kuroshio current during the observation period based on the Quick Bulletin of Ocean Conditions

4 Application to observations

4.1 Vertical distribution of ammonium concentration

The nanomolar level ammonium concentrations were investigated in the vicinity of the Kuroshio Current along 138°E (the O-line) in summer (September 2012) during the *R/V Soyo-maru* cruise (Fig. 9) to confirm the highly sensitive

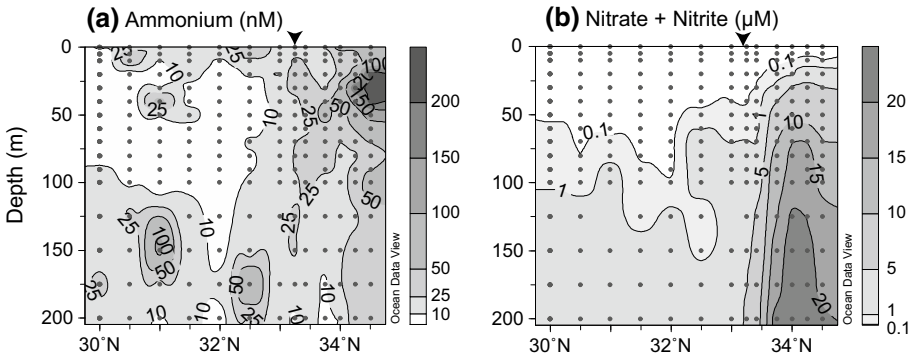

Fig. 10 Vertical distributions of **a** ammonium concentration and **b** nitrate + nitrite concentration. The *arrowheads* above the panels denote the position of the Kuroshio axis

analysis results for oceanic observations. The Kuroshio axis exists at 33°15′N based on the Quick Bulletin of the Ocean Conditions published by the Japanese Coast Guard (http://www1.kaiho.mlit.go.jp/KANKYO/KAIYO/qboc/index_E.html). Samples for ammonium concentration determination were collected using a Rosette Niskin attached to a CTD system (Seabird) at depths ranging from 5 m to 200 m, and immediately analyzed on board. The concentrations of other nutrients (nitrate, nitrite, silicate, and phosphate) were determined at an on land laboratory with a TrAAcs 2000 system (Bran + Luebbe) by conventional methods using stored (frozen) samples.

The minimum detection limit was 6 nM at a wavelength of 630 nm during the observations. The ammonium concentrations measured on board varied from <6 to 253 nM during the cruise (Fig. 10). Typical vertical profiles for ammonium concentration were obtained. The maximum subsurface ammonium concentration was just below the subsurface chlorophyll maximum (data not shown), and nitracline was the same as the oligotrophic Atlantic (Brzezinski 1988; Rees et al. 2006) (Fig.10). These results indicated that our system could be applied for ocean observations to understand the distributions of nanomolar level ammonium concentration in the oligotrophic ocean.

4.2 Measurement of ammonium excretion rate by zooplankton

This highly sensitive analysis method has potential for evaluation of the zooplankton excretion rate by zooplankton because it allows short-term and low-density incubations, which are insulated from the influence of starvation and stress of crowds (Steinberg and Saba 2008). Ammonium excretion by two different species of female adult copepods, *Calanus jashnovi* [prosoma length (PL) 3.18 ± 0.07 mm (mean ± SD), $n = 6$] and *Oncaea venusta* (PL: 0.65 ± 0.08 mm, $n = 12$), was measured during an early spring cruise (March 2013) along the O-line. The zooplankton were gently collected by a NORPAC net at 31°N and 33°45′N, immediately and individually sorted to 13 mL filtered in situ surface seawater, and incubated for approximately 4 h in darkness at the in situ sea surface temperature (18 °C).

The ammonium concentration increased to 2,680 ± 70 nM and 184 ± 107 nM for the incubated bottles of *C. jashnovi* and *O. venusta* from the control bottles (with only filtered in situ surface seawater), respectively. The excretion rates were 116 ± 7 and 7.2 ± 4.8 ng N h^{-1} ind^{-1} by *C. jashnovi* and *O. venusta*, respectively. These values were the same order of magnitude as the reported values from the same temperature range but with different zooplankton species (Ikeda et al. 2001). Therefore, this method was used for the estimation of short-term ammonium excretion rates by copepods, which are approximately two-orders of magnitude different by species and/or sizes, because the present method can measure a four-order range of ammonium concentration.

5 Conclusions

The present method provides a highly sensitive technique for analyzing a wide range of ammonium concentrations in seawater. This system may be applied for different kinds of oceanic observations and experiments because it is based on existing and commercially available systems, which can detect nanomolar and micromolar concentrations of ammonium. In addition, deionized water was determined as an acceptable blank solution. Thus, unified blank and working standards can be utilized for ammonium analysis. Furthermore, a continuous flow autoanalyzer equipped with LWCCs was applied for the continuous determination of nanomolar concentrations of nitrate, phosphate, and silicate in the oceanic surface water. This method provided clear horizontal distributions and spatial variations of nutrient concentrations in oligotrophic oceans (Hashihama et al. 2009, 2010, 2014; Kodama et al. 2011). This new highly sensitive analytical method for ammonium determination may also be used to detect the horizontal distribution of ammonium concentrations along with other nutrients, thus,

making major contributions to the understanding of nitrogen dynamics in oligotrophic oceans.

Acknowledgments We thank the officers and crewmembers of the *R/V Soyo-maru Koda* cruise for their cooperation at sea. We are grateful to Mr. H. Kikuchi of BL-TEC for his technical assistance and advice. This work was financially supported by the Ministry of Agriculture, Forestry and Fisheries, Japan through a research project entitled "Development of technologies for mitigation and adaptation to climate change in Agriculture, Forestry and Fisheries" and by a MEXT grant (24121005) to K. F.

References

Amornthammarong N, Zhang JZ (2008) Shipboard fluorometric flow analyzer for high-resolution underway measurement of ammonium in seawater. Anal Chem 80(4):1019–1026. doi:10.1021/ac701942f

Bronk DA (2002) Dynamics of DON. In: Hansell DA, Carlson CA (eds) Biogeochemistry of marine dissolved organic matter. Academic Press, San Diego, pp 153–247. doi:10.1016/B978-012323841-2/50007-5

Brzezinski MA (1987) Colorimetric determination of nanomolar concentrations of ammonium in seawater using solvent-extraction. Mar Chem 20(3):277–288. doi:10.1016/0304-4203(87)90078-8

Brzezinski MA (1988) Vertical distribution of ammonium in stratified oligotrophic waters. Limnol Oceanogr 33(5):1176–1182. doi:10.4319/lo.1988.33.5.1176

Chen GH, Zhang M, Zhang Z et al (2011) On-line solid phase extraction and spectrophotometric detection with flow technique for the determination of nanomolar level Ammonium in seawater samples. Anal Lett 44(1–3):310–326. doi:10.1080/00032719.2010.500775

Clark DR, Rees AP, Joint I (2007) A method for the determination of nitrification rates in oligotrophic marine seawater by gas chromatography/mass spectrometry. Mar Chem 103(1–2):84–96. doi:10.1016/j.marchem.2006.06.005

Coverly S, Kerouel R, Aminot A (2012) A re-examination of matrix effects in the segmented-flow analysis of nutrients in sea and estuarine water. Anal Chim Acta 712:94–100. doi:10.1016/j.aca.2011.11.008

Dean JA (1998) Lange's handbook of chemistry. McGraw-Hill Inc, New York

Dortch Q (1990) The interaction between ammonium and nitrate uptake in phytoplankton. Mar Ecol Prog Ser 61(1–2):183–201. doi:10.3354/Meps061183

Eppley RW, Peterson BJ (1979) Particulate organic matter flux and planktonic new production in the deep ocean. Nature 282(5740):677–680. doi:10.1038/282677a0

Francis CA, Roberts KJ, Beman JM et al (2005) Ubiquity and diversity of ammonia-oxidizing archaea in water columns and sediments of the ocean. Proc Nat Acad Sci 102(41):14683–14688. doi:10.1073/pnas.0506625102

Garside C (1982) A chemiluminescent technique for the determination of nanomolar concentrations of nitrate and nitrite in seawater. Mar Chem 11(2):159–167. doi:10.1016/0304-4203(82)90039-1

Gordon LI, Jennings Jr JC, Ross AA et al (1993) A suggested protocol for continuous flow automated analysis of seawater nutrients (phosphate, nitrate, nitrite and silicic acid) in the WOCE hydrographic program and the joint global ocean fluxes study. WOCE Operations Manual, WHP Office Report WHPO 91-1, WOCE Report No. 68/91. Woods Hole, Massachusetts, USA

Harrison WG, Harris LR, Irwin BD (1996) The kinetics of nitrogen utilization in the oceanic mixed layer: nitrate and ammonium interactions at nanomolar concentrations. Limnol Oceanogr 41(1):16–32. doi:10.4319/lo.1996.41.1.0016

Hashihama F, Kanda J (2010) Automated colorimetric determination of trace silicic acid in seawater by gas-segmented continuous flow analysis with a liquid waveguide capillary cell. La mer 47:119–127

Hashihama F, Furuya K, Kitajima S et al (2009) Macro-scale exhaustion of surface phosphate by dinitrogen fixation in the western North Pacific. Geophys Res Lett vol 36. doi:10.1029/2008gl036866

Hashihama F, Sato M, Takeda S et al (2010) Mesoscale decrease of surface phosphate and associated phytoplankton dynamics in the vicinity of the subtropical South Pacific islands. Deep-Sea Res I 57(3):338–350. doi:10.1016/j.dsr.2009.12.005

Hashihama F, Kanda J, Maeda Y et al (2014) Selective depressions of surface silicic acid within cyclonic mesoscale eddies in the oligotrophic western North Pacific. Deep Sea Res I 90:115–124. doi:10.1016/j.dsr.2014.05.004

Hydes D, Aoyama M, Aminot A et al (2010) Determination of dissolved nutrients (N, P, Si) in seawater with high precision and inter-comparability using gas-segmented continuous flow analysers. In: The GO-SHIP Repeat Hyrography Manual: a collection of expert reports and guidelines, IOCCP report No. 14, ICPO publication series No. 134, version 1

Ikeda T, Kanno Y, Ozaki K et al (2001) Metabolic rates of epipelagic marine copepods as a function of body mass and temperature. Mar Biol 139(3):587–596. doi:10.1007/s00227-001-0743-z

Jones RD (1991) An improved fluorescence method for the determination of nanomolar concentrations of ammonium in natural waters. Limnol Oceanogr 36(4):814–819. doi:10.4319/lo.1991.36.4.0814

Karl DM, Tien G (1992) MAGIC: a sensitive and precise method for measuring dissolved phosphorus in aquatic environments. Limnol Oceanogr 37(1):105–116. doi:10.4319/lo.1992.37.1.0105

Karl DM, Letelier R, Hebel DV et al (1992) *Trichodesmium* blooms and new nitrogen in the North Pacific gyre, marine pelagic cyanobacteria: *Trichodesmium* and other diazotrophs. Springer, Berlin, pp. 219–237

Kerouel R, Aminot A (1997) Fluorometric determination of ammonia in sea and estuarine waters by direct segmented flow analysis. Mar Chem 57(3–4):265–275. doi:10.1016/S0304-4203(97)00040-6

Kirchman DL, Keil RG, Wheeler PA (1990) Carbon limitation of ammonium uptake by heterotrophic Bacteria in the SubArctic Pacific. Limnol Oceanogr 35(6):1258–1266. doi:10.4319/lo.1990.35.6.1258

Kodama T, Furuya K, Hashihama F et al (2011) Occurrence of rain-origin nitrate patches at the nutrient-depleted surface in the East China Sea and the Philippine Sea during summer. J Geophys Res Oceans 116:C08003. doi:10.1029/2010jc006814

Li QP, Hansell DA (2008) Intercomparison and coupling of magnesium-induced co-precipitation and long-path liquid-waveguide capillary cell techniques for trace analysis of phosphate in seawater. Anal Chim Acta 611(1):68–72. doi:10.1016/j.aca.2008.01.074

Li QP, Zhang JZ, Millero FJ et al (2005) Continuous colorimetric determination of trace ammonium in seawater with a long-path liquid waveguide capillary cell. Mar Chem 96(1–2):73–85. doi:10.1016/j.marchem.2004.12.001

Lipschultz F (2001) A time-series assessment of the nitrogen cycle at BATS. Deep Sea Res II 48(8–9):1897–1924. doi:10.1016/S0967-0645(00)00168-5

Ma J, Adornato L, Byrne RH et al (2014) Determination of nanomolar levels of nutrients in seawater. Trends Anal Chem 60:1–15. doi:10.1016/j.trac.2014.04.013

Matsumoto K, Furuya K, Kawano T (2004) Association of picophytoplankton distribution with ENSO events in the equatorial Pacific between 145°E and 160°W. Deep Sea Res I 51(12):1851–1871. doi:10.1016/j.dsr.2004.07.015

McCarthy MD, Bronk DA (2008) Analytical methods for the study of nitrogen. In: DG Capone, EJ Carpenter, DA Bronk et al (eds) Nitrogen in the marine environment. Academic, London, pp. 1220–1271. doi:10.1016/B978-0-12-372522-6.00028-1

Miller JC, Miller JN (1988) Statistics for analytical chemistry. Ellis Horwood series in analytical chemistry. E. Horwood, New York

Nishino S, Itoh M, Kawaguchi Y et al (2011) Impact of an unusually large warm-core eddy on distributions of nutrients and phytoplankton in the southwestern Canada Basin during late summer/early fall 2010. Geophys Res Lett vol 38. doi:10.1029/2011gl047885

O'Connor Šraj L, Almeida M, Swearer SE et al (2014) Analytical challenges and advantages of using flow-based methodologies for ammonia determination in estuarine and marine waters. Chem, Trends Anal. doi:10.1016/j.trac.2014.03.012

Oliveira SM, Marques da Silva Lopes TI, Toth IV et al (2009) Determination of ammonium in marine waters using a gas diffusion multicommuted flow injection system with in-line prevention of metal hydroxides precipitation. J Environ Monit 11(1):228–234. doi:10.1039/b812624k

Parsons TR, Maita Y, Lalli CM (1984) A manual of chemical and biological methods for seawater analysis. Pergamon, Oxford

Patey MD, Rijkenberg MJA, Statham PJ et al (2008) Determination of nitrate and phosphate in seawater at nanomolar concentrations. Trends Anal Chem 27(2):169–182. doi:10.1016/j.trac.2007.12.006

Plant JN, Johnson KS, Needoba JA et al (2009) NH_4-Digiscan: an in situ and laboratory ammonium analyzer for estuarine, coastal, and shelf waters. Limnol Oceanogr Methods 7:144–156. doi:10.4319/lom.2009.7.144

Raimbault P, Garcia N (2008) Evidence for efficient regenerated production and dinitrogen fixation in nitrogen-deficient waters of the South Pacific Ocean: impact on new and export production estimates. Biogeosciences 5(2):323–338. doi:10.5194/bg-5-281-2008

Raimbault P, Garcia N, Cerutti F (2008) Distribution of inorganic and organic nutrients in the south Pacific Ocean—evidence for long-term accumulation of organic matter in nitrogen-depleted waters. Biogeosciences 5(2):281–298. doi:10.5194/bg-5-311-2008

Rees AP, Woodward EMS, Joint I (2006) Concentrations and uptake of nitrate and ammonium in the Atlantic Ocean between 60°N and 50°S. Deep Sea Res II 53(14–16):1649–1665. doi:10.1016/j.dsr2.2006.05.008

Saino T, Otobe H, Wada E et al (1983) Subsurface ammonium maximum in the northern North Pacific and the Bering Sea in summer. Deep Sea Res A 30(11):1157–1171. doi:10.1016/0198-0149(83)90094-8

Schulze G, Liu C, Brodowski M et al (1988) Different approaches to the determination of ammonium ions at low levels by flow injection analysis. Anal Chim Acta 214:121–136. doi:10.1016/S0003-2670(00)80435-3

Steinberg DK, Saba GK (2008) Nitrogen consumption and metabolism in marine zooplankton. In: Capone DG, Carpenter EJ, Bronk DA et al (eds) Nitrogen in the marine environment. Academic, London, pp 1135–1196. doi:10.1016/B978-0-12-372522-6.00026-8

Van Son M, Schothorst R, Den Boef G (1983) Determination of total ammoniacal introgen in water by flow injection analysis and a gas diffusion membrane. Anal Chim Acta 153:271–275. doi:10.1016/S0003-2670(00)85513-0

Ward BB (2011) Measurement and distribution of nitrification rates in the oceans. Meth Enzymol 486:307–323. doi:10.1016/B978-0-12-381294-0.00013-4

Wheeler PA, Kirchman DL (1986) Utilization of inorganic and organic nitrogen by bacteria in marine systems. Limnol Oceanogr 31(5):998–1009. doi:10.4319/lo.1986.31.5.0998

Zhu Y, Yuan DX, Huang YM et al (2014) A modified method for on-line determination of trace ammonium in seawater with a long-path liquid waveguide capillary cell and spectrophotometric detection. Mar Chem 162:114–121. doi:10.1016/j.marchem.2014.03.011